Charm @t CMS

Jhovanny Andres Mejia Guisao
On behalf of the CMS collaboration
UNIVERSIDAD DE ANTIOQUIA, COLOMBIA

**CHARM2020: 10th International Workshop on Charm Physics,
31 May-4 Jun 2021, Mexico City.**

Outline

Physics results

★ **Observation of the Bs→X(3872)ϕ decay.**
CMS-BPH-17-005, Phys. Rev. Lett. 125 (2020) 152001

★ **Measurement of prompt open-charm production cross sections in proton-proton collisions at 13 TeV.**
CMS-PAS-BPH-18-003

★ **Discovery of the Bc(2S) and Bc*(2S) states.**
Phys. Rev. Lett. 122 (2019) 132001, Phys. Rev. D 102 (2020) 092007
Dedicated talk by Daniel Alejandro PÉREZ

The CMS experiment

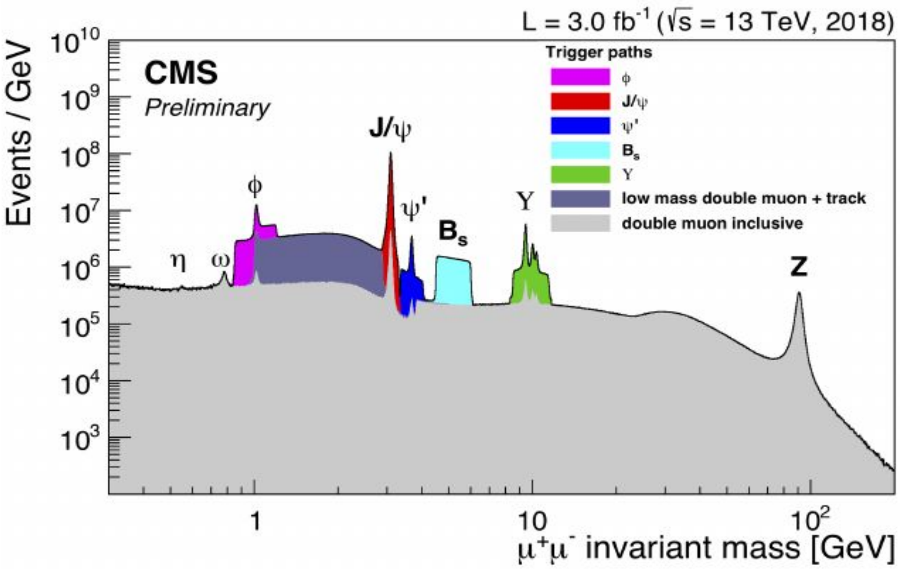

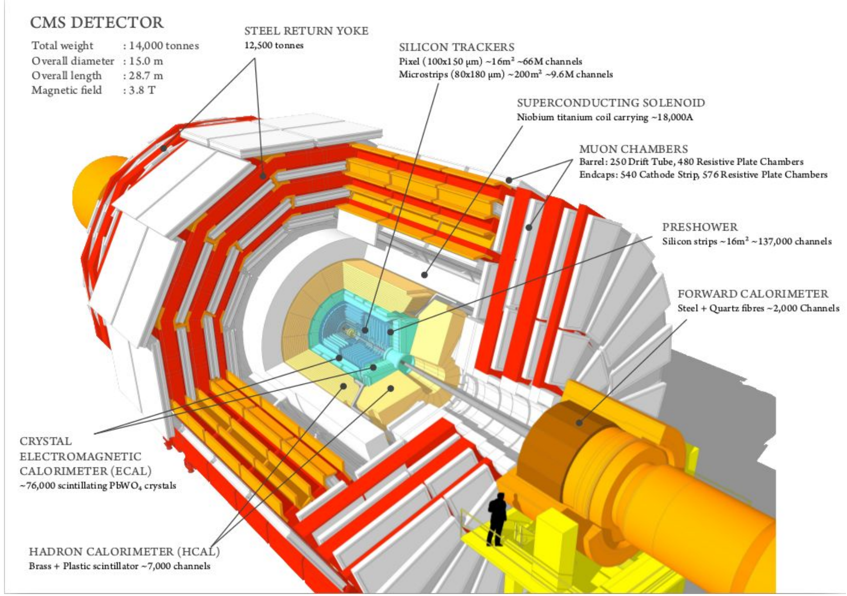

- The CMS Experiment at the LHC was designed mainly for high-pT physics (Higgs, top-quark, SM precision measurement, New Physics searches etc)

- However, a robust muon system, good pT resolution and excellent vertex reconstruction provide promising opportunities for heavy flavour and quarkonia-related analyses.

CMS-BPH-17-005, Phys. Rev. Lett. 125 (2020) 152001:

Observation of the $B_s \to X(3872)\phi$ decay

Exotic Hadrons

- ➔ From 2003, thanks to B-factories Belle and BaBar (and then BES III and LHCb), the number of the candidates to exotic hadrons is growing continuously.
  These are multiquark states. Some bright examples are: **X(3872)** and **Z(4430)+** from Belle, **X(4260)** from BaBar, **Z(3900)+** from BESIII /Belle

- ➔ X(3872) was observed in 2003 by Belle, but its nature is still unclear.

- ➔ **J^{pc} = 1^{++}** corresponds to charmonium χ_{c1}, PDG calls it " **χ_{c1}(3872), also known as X(3872)** "

- ➔ Many theoretical interpretations exist, e.g. **tetraquark, molecule, or mixture of those with a conventional charmonium state.**

- ➔ Measurement of its production in **Bs** decays helps understanding the properties of **X(3872)**, in particular dynamics of its formation in **B hadron decays.**

$$R \equiv \frac{\mathcal{B}[B_s^0 \to X(3872)\phi]\mathcal{B}[X(3872) \to J/\psi\pi^+\pi^-]}{\mathcal{B}[B_s^0 \to \psi(2S)\phi]\mathcal{B}[\psi(2S) \to J/\psi\pi^+\pi^-]} = \frac{N[B_s^0 \to X(3872)\phi]}{N[B_s^0 \to \psi(2S)\phi]}\frac{\epsilon_{B_s^0\to\psi(2S)\phi}}{\epsilon_{B_s^0\to X(3872)\phi}}$$

Datasets and Selection

- 140 fb^{-1} from collision dataset 2016-2018 (Run2 pp).
- Full decay reconstruction using inner detector and muon detectors:
  - triggers based on $\mathbf{J/\psi \to \mu^+\mu^-}$ identification
  - **Bs** Vertex fit performed with **J/ψ** mass constraint.
  - **Bs** Prob(vtx) > 0.07 (7%)
  - Lxy/σ_{Lxy}>15.0 (**Bs**(vtx)->PV)
  - **pT($K^{\pm}$)**>1.5 and 2.2 GeV
  - **pT($\pi^{\pm}$)**>0.7 GeV

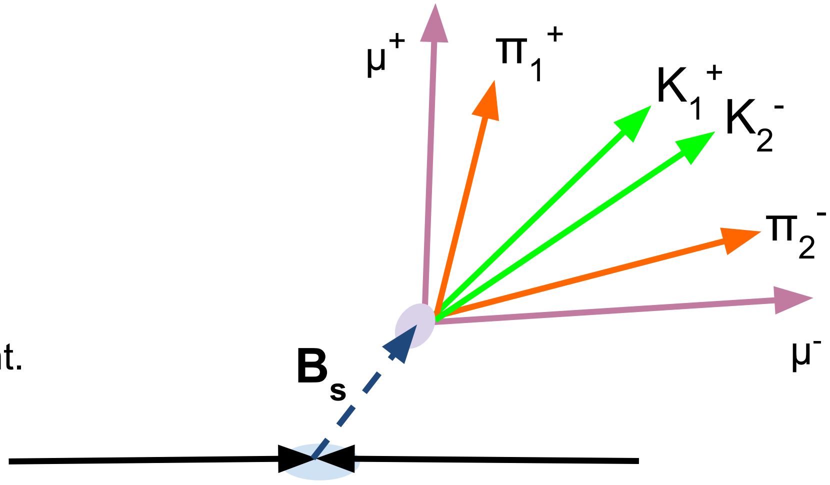

$\mathbf{B_s \to X(3872)\phi}$

M(ππ)> 0.7 GeV for the **X(3872)** channel

M(ππ)> 0.45 GeV for the **ψ(2S)** channel

3.60 **< M(J/Ψππ)** **<** 3.95 GeV (cober **X(3872)** and **Ψ(2S)**)

1.00 **< M(KK)** **<** 1.04 GeV

5.32 **< M(J/ΨππKK)** **<** 5.42 GeV

Yield Extraction: Ψ(2S) normalization channel

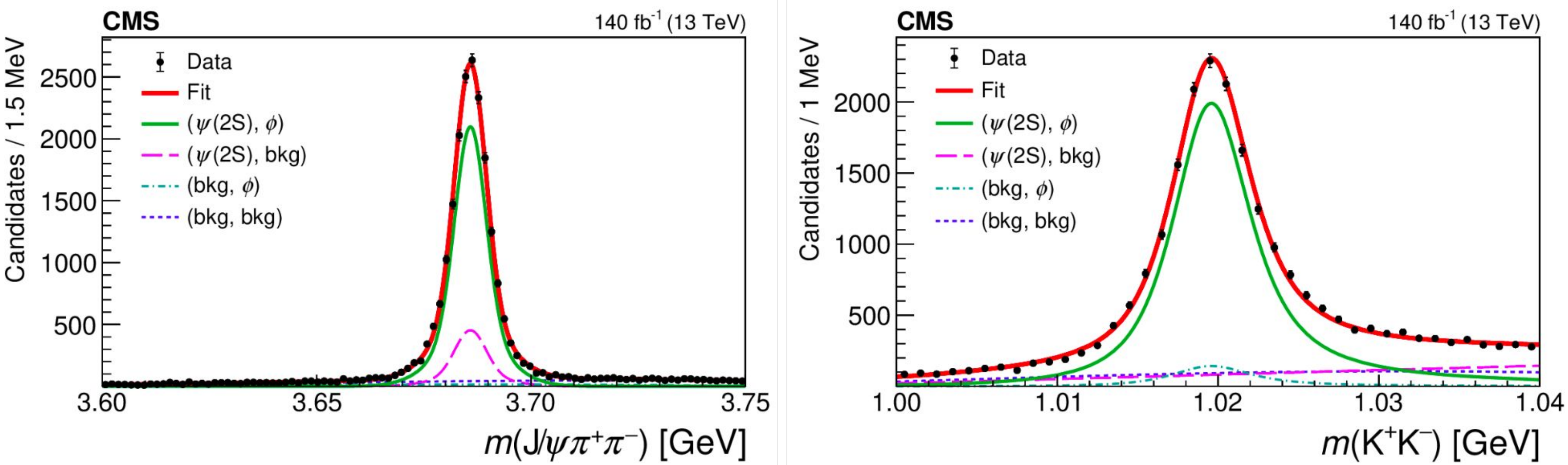

The B_s yields are extracted using a two-dimensional (2D) maximum likelihood fit. **M(J/Ψππ):M(KK)**

- ➔ **Ψ(2S) Signal model:** Double Gaussian(DG) with common mean.
- ➔ **Ψ(2S) Background model:** $(Z-Z_0)^{\beta} \times Pol_1(Z)$
- ➔ **ϕ Signal model:** RBW convolved with DG.
- ➔ **ϕ Background model:** $(Y-Y_0)^{\delta} \times Pol_1(Y)$

The fitted yield for the $B_s \to \Psi(2S)\phi$ component is: 15359 ± 171

Yield Extraction: X(3872) channel

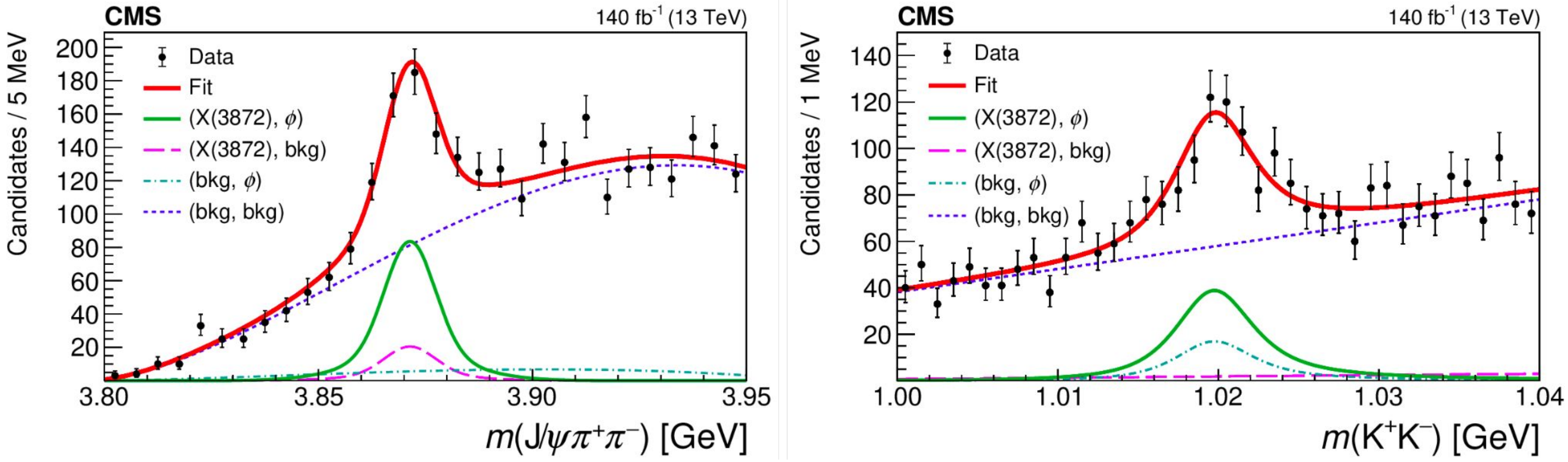

- ➢ The same fit function is used as in the **Ψ(2S)** channel. The shape of the **X(3872)** signal is fixed to the one obtained in data for **Ψ(2S)**, leaving free to float only a resolution scaling factor.
- ➢ Statistical significance **> 6σ**(systematics are included).

The fitted yield for the $B_s \to X(3872)\phi$ component is: 299 ± 39

Ratio of efficiencies $\epsilon_{B_s^0 \to \psi(2S)\phi} / \epsilon_{B_s^0 \to X(3872)\phi} = 1.136 \pm 0.026$

M(Bs) bkg-subtracted

- ➢ Evaluation of the residual non **Bs** background (non-**Bs** production of X(3872)phi) by using the non-resonant **bkg-subtracted M(X(3872)ϕ)** obtained by means of the **sPlot technique**. This bkg contribution is **1.7% (0.5% for Ψ(2S)ϕ)**.
- ➢ **It is use as systematic uncertainty**.

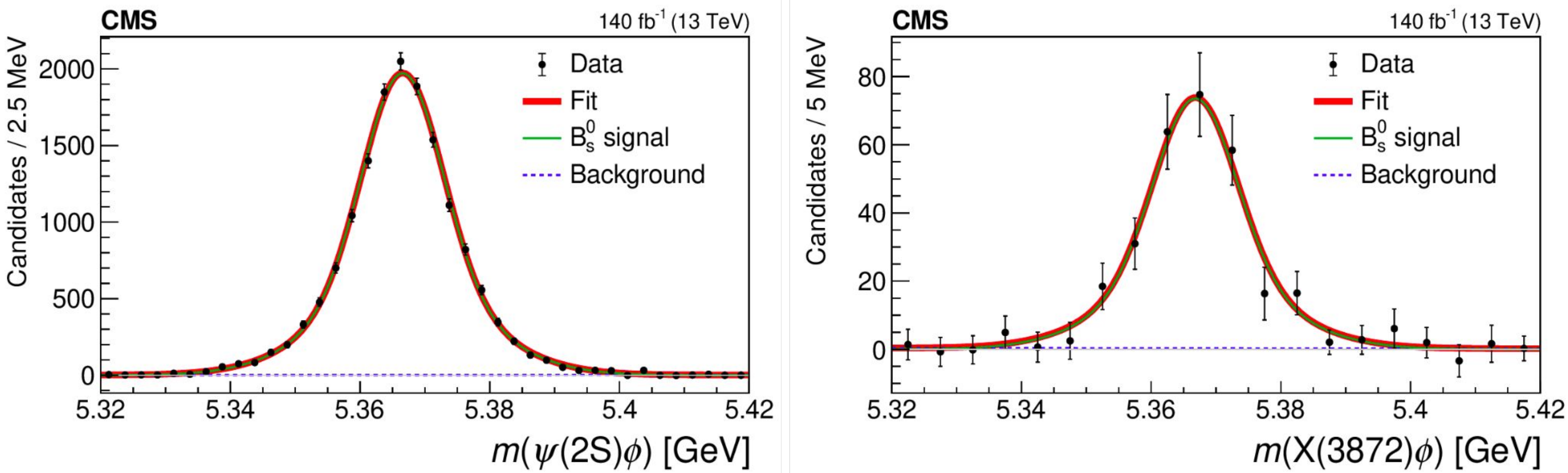

The systematic uncertainties

Relative systematic uncertainties in the ratio

$$= \frac{N[B_s^0 \to X(3872)\phi]}{N[B_s^0 \to \psi(2S)\phi]} \frac{\epsilon_{B_s^0 \to \psi(2S)\phi}}{\epsilon_{B_s^0 \to X(3872)\phi}}$$

Source	Uncertainty (%)
$m(K^+K^-)$ signal model	< 0.1
$m(K^+K^-)$ background model	2.5
$m(J/\psi\pi^+\pi^-)$ signal model	5.3
$m(J/\psi\pi^+\pi^-)$ background model	4.3
Non-B_s^0 background	1.2
Simulated sample size	2.2
Total	7.7

Results

Decay $B_s \to X(3872)\phi$ was observed for the first time

$$R \equiv \frac{\mathcal{B}[B_s^0 \to X(3872)\phi]\mathcal{B}[X(3872) \to J/\psi\pi^+\pi^-]}{\mathcal{B}[B_s^0 \to \psi(2S)\phi]\mathcal{B}[\psi(2S) \to J/\psi\pi^+\pi^-]} = [2.21 \pm 0.29(\mathrm{stat}) \pm 0.17(\mathrm{syst})]\%$$

Multiplying the measured ratio R by the known branching fractions

$$\mathcal{B}(B_s^0 \to X(3872)\phi)\,\mathcal{B}(X(3872) \to J/\psi\,\pi^+\pi^-) = (4.14 \pm 0.54\,(\mathrm{stat}) \pm 0.32\,(\mathrm{syst}) \pm 0.46\,(\mathcal{B})) \times 10^{-6}$$

This branching fraction product can be compared to similar ones in B^0 and B^+ decays

$B^0 \to X K^0$	$(4.3 \pm 1.3)\times10^{-6}$
$B^0 \to X K^*(892)^0$	$(4.0 \pm 1.5)\times10^{-6}$
$B^+ \to X K^+$	$(8.6 \pm 0.8)\times10^{-6}$

$B_s \to X\phi$ $(4.14 \pm 0.78)\times10^{-6}$ (CMS)

The measured value for B_s is consistent with that for B^0 but about two times smaller than the one for B^+

$$\frac{\mathcal{B}(B_s^0 \to X(3872)\phi)}{\mathcal{B}(B^+ \to X(3872)K^+)} = 0.482 \pm 0.063\,(\mathrm{stat}) \pm 0.037\,(\mathrm{syst}) \pm 0.070\,(\mathcal{B})$$

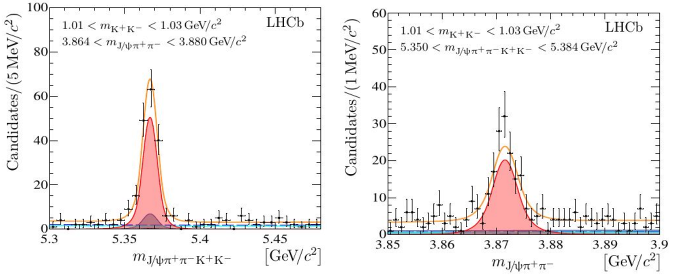

JHEP 02 (2021) 024

$$\mathcal{R}^{\chi_{c1}(3872)\phi}_{\psi(2S)\phi} = (2.42 \pm 0.23 \pm 0.07) \times 10^{-2}$$

Comparison to other measurements

➔ This suggests a **difference** in the production dynamics of the exotic **X(3872)** in **B^0 and B_s** decays compared to **B^+** with respect to the standard **Ψ(2S)**.

➔ This observation may help in the comprehension of the **nature of X(3872)**.

➔ An explanation of the observed difference in the decay branching fractions has been proposed within the **tetraquark picture of the X(3872)state**: "***The established decay pattern, including the up-to-date observations by CMS, are explained by the mixing of two quasidegenerate, unresolvable neutral states***" **[Maiani et al., PRD 102 (2020) 034017]**

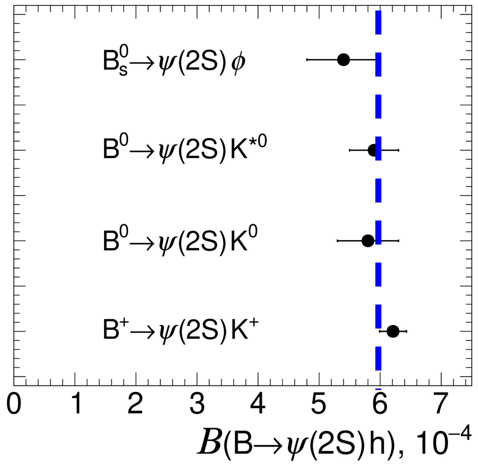

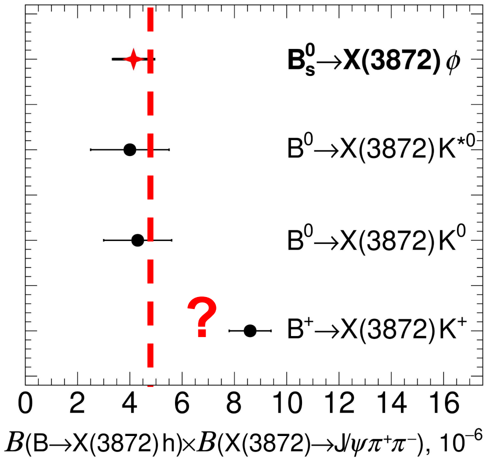

CMS-PAS-BPH-18-003

Measurement of prompt open-charm production cross sections in proton-proton collisions at 13 TeV.

Motivation for open-charm production measurements

Although quantum chromodynamics (QCD) is well established as the theory of the strong interaction, a complete understanding of the (nonperturbative) processes that lead to the binding of quarks and gluons into hadrons is still lacking.

- ➔ Measurements provide **important tests of QCD** and give insight into particle production at colliders.

- ➔ **Current calculations suffer from large theoretical uncertainties**.
  - ◆ experimental constraints on **heavy-quark production cross sections** are relevant for all the physics phenomena for which heavy-quark production is an **important background process**.

- ➔ LHC provides access to **wide kinematic range** with a **very high production cross section** if compared to ee colliders.

Datasets and Selection

➢ **29 nb^{-1}** Run2 pp collision from dataset 2016.

➢ **ZeroBias trigger** applied (the most inclusive one)

➢ This analysis has been considered next decays channels:
   - $\mathbf{D^{*+} \rightarrow D^0 \pi_s \rightarrow K^- \pi^+ \pi_s}$
   - $\mathbf{D^0 \pi_s \rightarrow K^- \pi^+}$
   - $\mathbf{D^+ \rightarrow K^- \pi^+ \pi^+}$

➢ Phase space: **4 < pT(D) < 100** GeV && **|η| < 2.1**

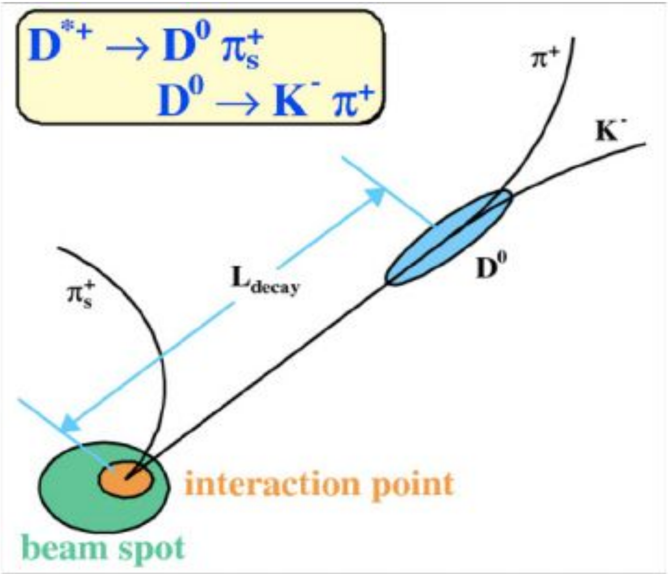

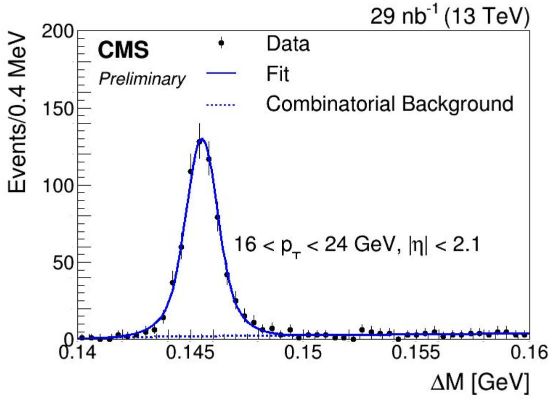

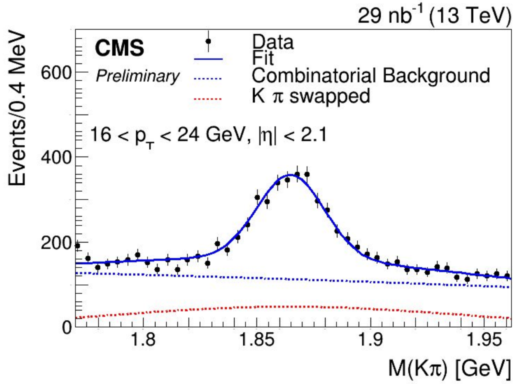

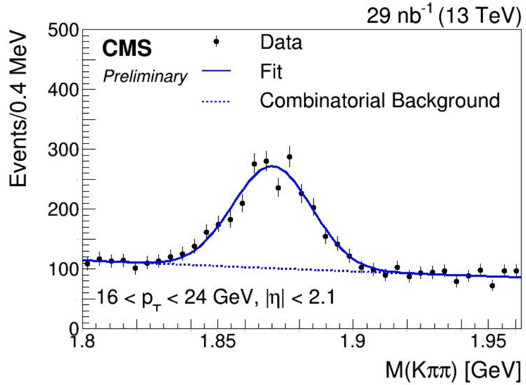

Selection

Variables	D^{*+}	D^0	D^+
PV selection:	largest $\sum p_T^2$	largest $\sum p_T^2$	largest $\sum p_T^2$
Tracks: ${p_T}^{min}$ [GeV]	0.5 (0.3 for the π_s)	0.8	0.7
Tracks: reduced χ^2	< 2.5 (3 for the π_s)	< 2.5	< 2.5
Tracks: N Tracker Hits	≥ 5 (> 2 for the π_s)	≥ 5	≥ 5
Tracks: N Pixel Hits	≥ 2 (none for the π_s)	≥ 2	≥ 2
Tracks: IP_{xy} [cm]	< 0.1 (sig. < 3 for π_s)	< 0.1	< 0.1
Tracks: IP_z [cm]	< 1 (sig. < 3 for π_s)	< 1	< 1
$\lvert M_{cand} - M^{PDG}\rvert$ [GeV]	< 0.023	< 0.10	< 0.10
SV fit CL	$> 1\%$	$> 1\%$	$> 1\%$
Pointing, $cos\Phi$	> 0.99	> 0.99	> 0.99
L significance:	> 3	> 5	> 10
Arbitration	min ΔM	min $\lvert M(K\pi) - M^{PDG}(D^0)\rvert$	min $\lvert M(K\pi\pi) - M^{PDG}(D^+)\rvert$

Contamination from secondary decay

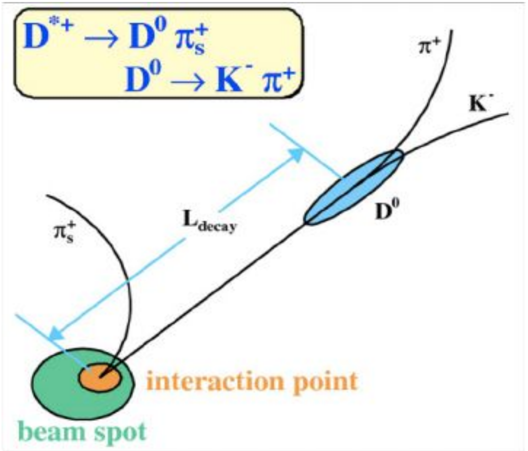

The aim of this analisys is to measure the **prompt open-charm production cross sections**

- **prompt = coming from PV or charm excited states**

It is important to evaluate and subtract the **contribution coming from nonprompt** charm mesons **arising from b hadron decays.**

The contamination rate is quantified using MC:

$$\text{contam} = N_{sec}/(N_{sec}+N_{prompt}) \sim 5\text{-}17\ \%$$

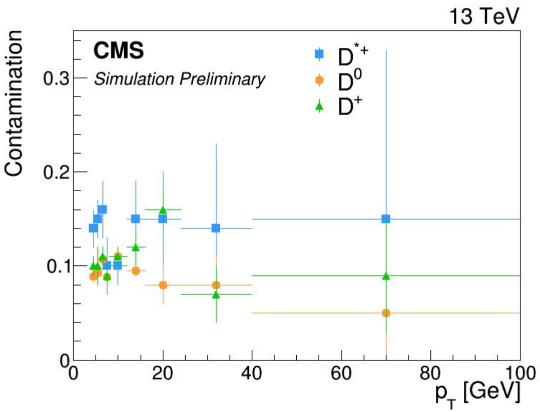

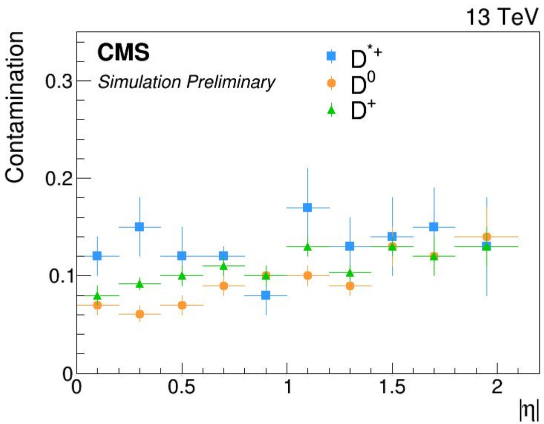

The systematic uncertainties

Systematic uncertainties for differential cross sections

$$\frac{d\sigma(pp \to DX)}{dp_T} = \frac{N_i(D \to f)}{\Delta p_T \mathcal{B}(D \to f) \mathcal{L} \varepsilon_{i,tot}(D \to f)}$$

$$\frac{d\sigma(pp \to DX)}{d|\eta|} = \frac{N_i(D \to f)}{\Delta \eta \mathcal{B}(D \to f) \mathcal{L} \varepsilon_{i,tot}(D \to f)}$$

	D^{*+}	D^0	D^+
Signal efficiency calculation	0.3	0.3	3.5
Secondary decay contamination	2.9	0.8	1.4
PU reweighting	1.0	1.0	2.0
Branching fraction	1.1	0.8	1.7
Tracking efficiency	9.4	4.2	6.1
Signal modeling	3.6	5.0	4.2
Background modeling	1.2	4.8	8.0
Luminosity	2.5	2.5	2.5
Time-dependent inefficiencies	1.4	1.4	1.4
Total	11.0	8.7	12.2

Results

The cross section values are compared to the predictions of next-to-leading-order plus next-to-leading-logarithmic accuracy (NLO+NLL) calculations by FONLL, and compared to different MC.

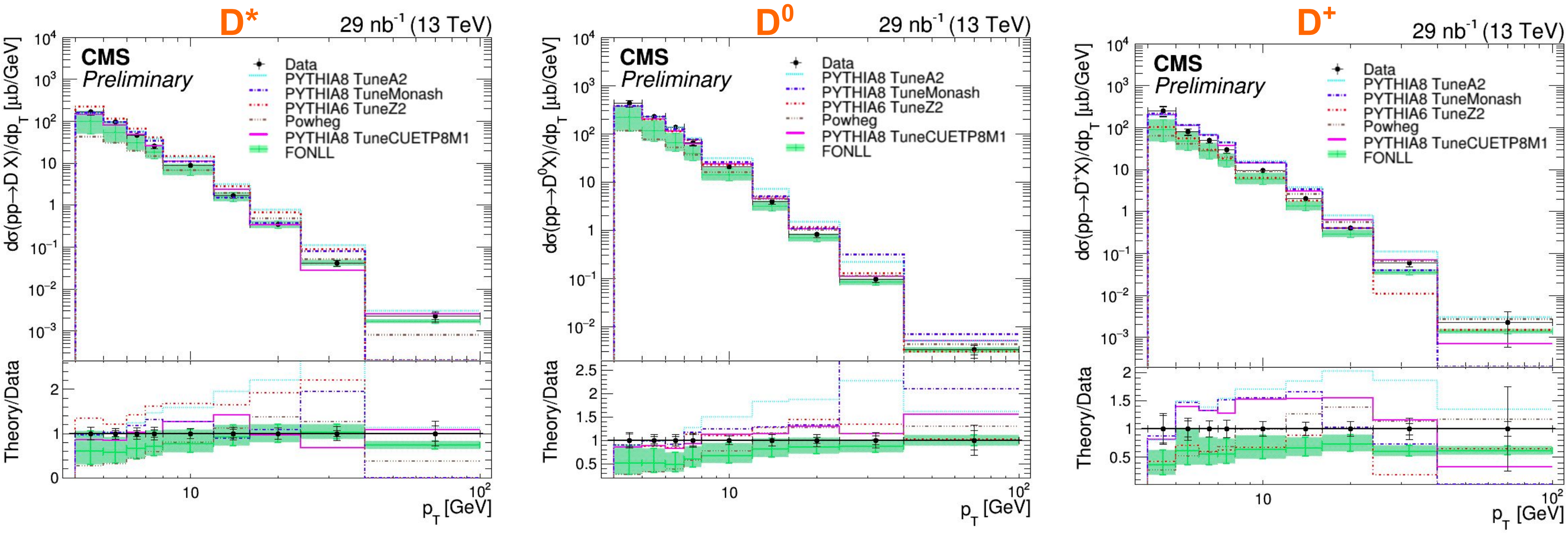

Comparison to other experiments: ATLAS

Since the ATLAS results include both prompt and nonprompt charm mesons, the correspoding FONLL predictions include both components as well.

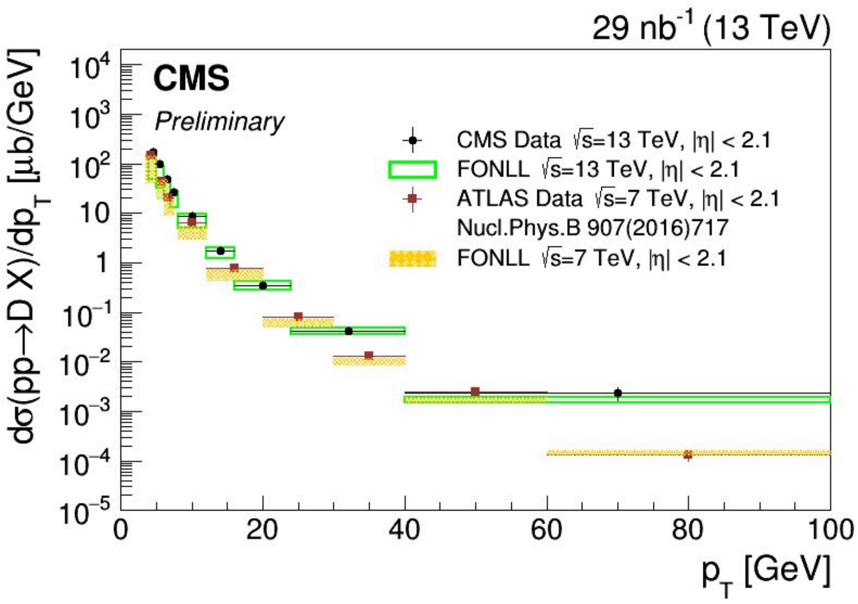

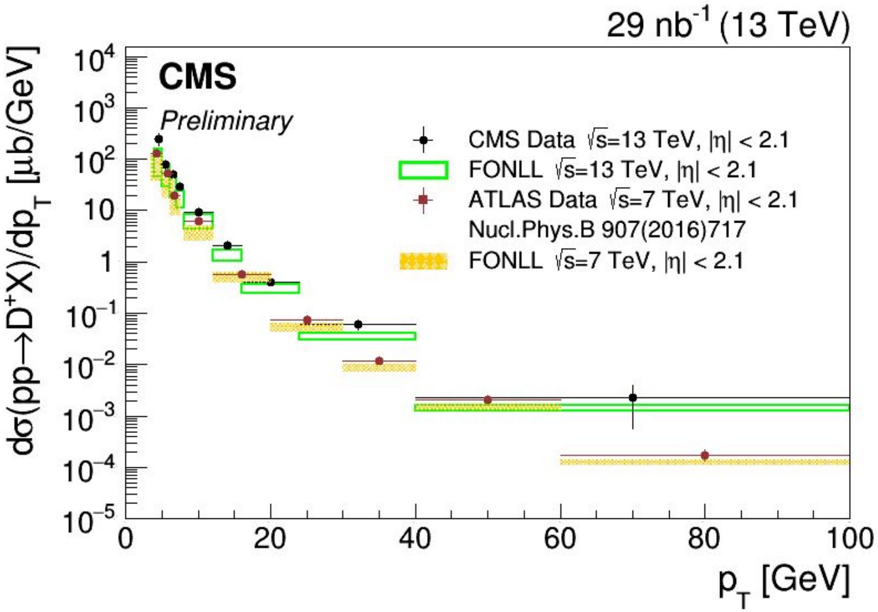

Comparison to other experiments: ALICE

Different kinematic range.
CMS data shown only for pT < 24 GeV.
Factor 2 in cross section since the cc are not included in ALICE

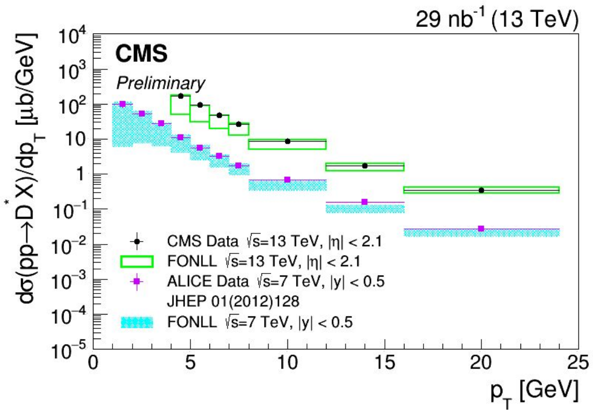

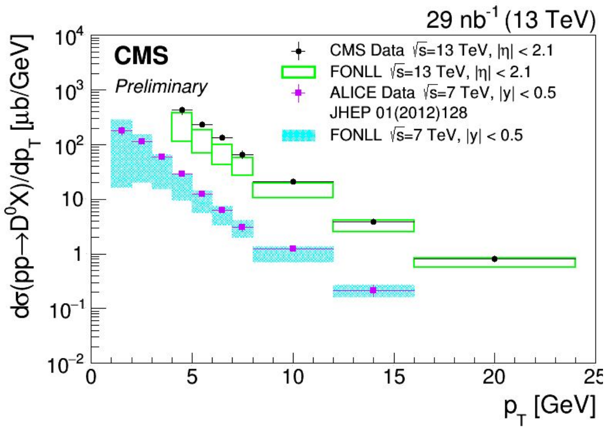

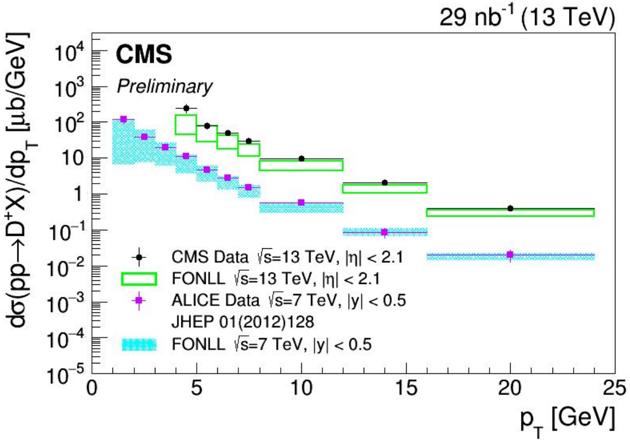

Comparison to other experiments: LHCb

Since the acceptances of the CMS and LHCb experiments differ, the two measurements are complementary and the results presented in this analisys extend the reconstruction to the rapidity region not covered by LHCb.

Only the first y bin is shown for LHCb.

CMS data are reported only for pT<16 GeV to have a better comparison.

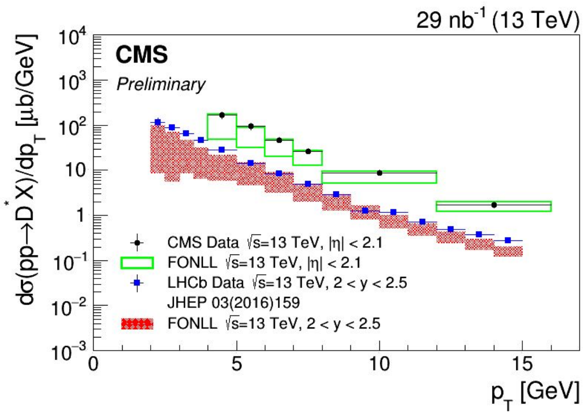

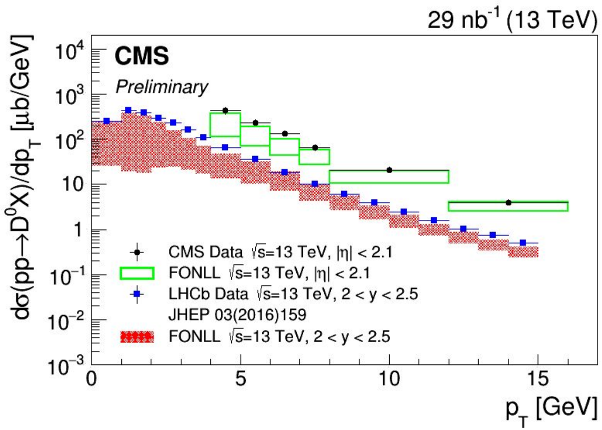

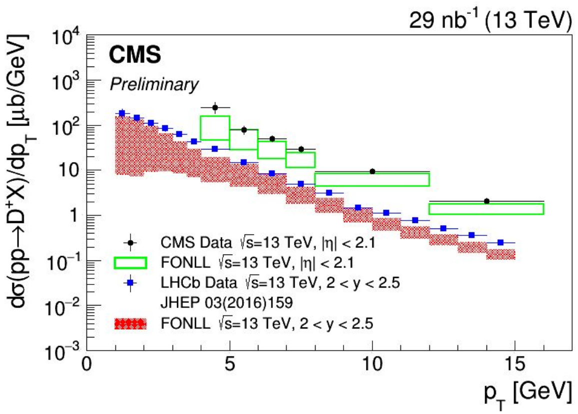

Summary

The $B_s \to X(3872)\phi$ decay was observed for the first time.

➔ Measured branching fraction is similar to B^0 , twice smaller than that of B^+

$$\frac{\mathcal{B}(B_s^0 \to X(3872)\phi)}{\mathcal{B}(B^+ \to X(3872)K^+)} = 0.482 \pm 0.063\,(\text{stat}) \pm 0.037\,(\text{syst}) \pm 0.070\,(\mathcal{B})$$

➔ The X(3872) production in B decays supports its non conventional nature.

The results on the first measurement of the open-charm production cross section in pp collision in CMS, using 2016 data, has been presented here.

CMS measurements show a good agreement with the previous ones within LHC. The measurements tend to favor a higher cross section than predicted by the FONLL calculations and smaller than estimated by the PYTHIA event generators.

Stay tuned for more updates!

Thanks!

Maiani et al., PRD 102 (2020) 034017

Assuming a tetraquark $X(3872)$, in the blob of Fig. 1 one has to create a light quark pair from the sea. The overall weak decay is

$$(\bar{b} + u, d, s)_{B^+, B^0, B_s} \to \bar{c} + c\bar{s} + (d\bar{d} \text{ or } u\bar{u})_{\text{sea}} + u, d, s.$$

The decays $B^{0,+} \to XK^{0,+}$ are then described by two amplitudes: A_1, where the $\bar{s}$ forms the kaon with the spectator u or d quark, and A_2, where it forms the kaon with a d or u quark from the sea. In terms of the unmixed states

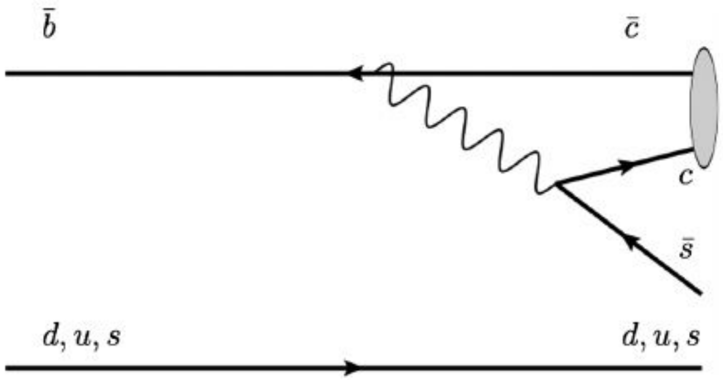

FIG. 1. The valence quarks in B and B_s decays. A pair of sea quarks is formed in the blob to generate the X tetraquarks.

$$\begin{aligned}
\mathcal{A}(B^0 \to X_d K^0) &\sim A_1 + A_2, \\
\mathcal{A}(B^0 \to X_u K^0) &\sim A_1, \\
\mathcal{A}(B^0 \to X^- K^+) &\sim A_2
\end{aligned} \quad (5)$$

$$\begin{aligned}
\mathcal{A}(B^+ \to X_d K^+) &\sim A_1, \\
\mathcal{A}(B^+ \to X_u K^+) &\sim A_1 + A_2, \\
\mathcal{A}(B^+ \to X^+ K^0) &\sim A_2.
\end{aligned} \quad (6)$$

Results

The cross section values are compared to the predictions of next-to-leading-order plus next-to-leading-logarithmic accuracy (NLO+NLL) calculations by FONLL, and compared to different MC.

D*

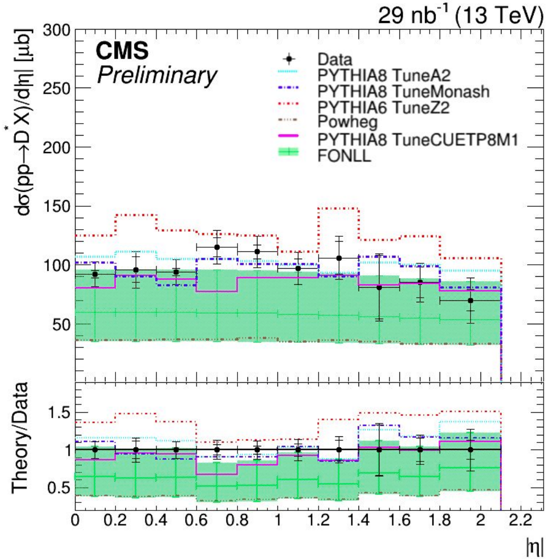

D^0

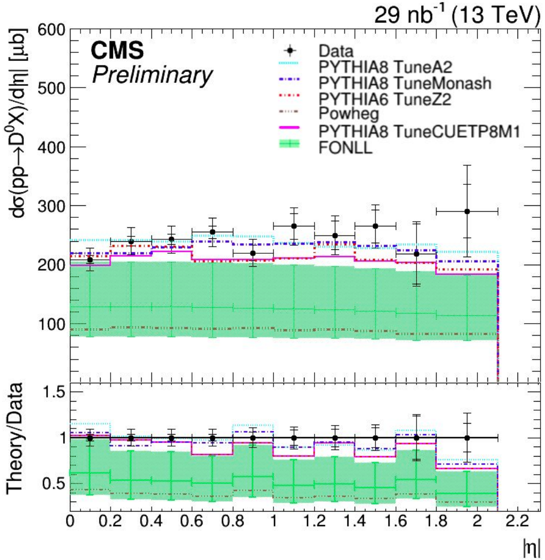

D$^+$

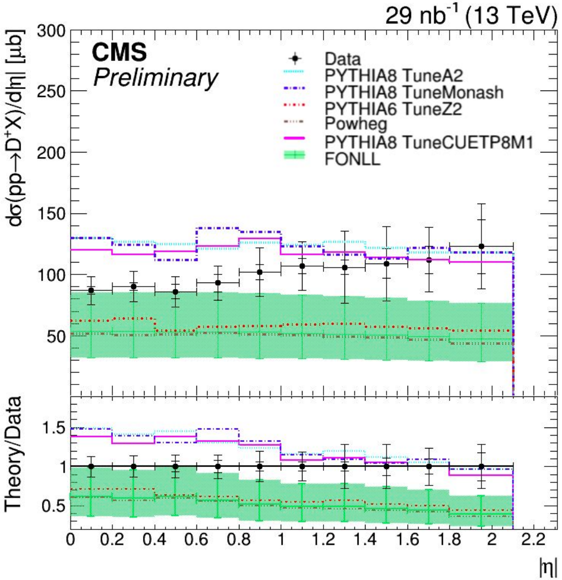

Comparison to other experiments: CMS (5.02 TeV)

Again, in both cases, a similar agreement between data and FONLL predictions is obtained.